

## Supporting Information

# Effects of Heating Rate on the Nucleation, Growth and Transformation of InOOH and In<sub>2</sub>O<sub>3</sub> via Solvothermal Reactions

Shunxi Tang, Jian Zhang,\* Si Wu, Chunyuan Hu, Yingai Li, Lina Jiang and Qiliang Cui

*State Key Laboratory of Superhard Materials, Jilin University, 130012 Changchun, P.R. China*

*\* Corresponding Author: E-mail: zhang\_jian@jlu.edu.cn; Fax: +86 431 85168346; Tel: +86*

*43185168881*

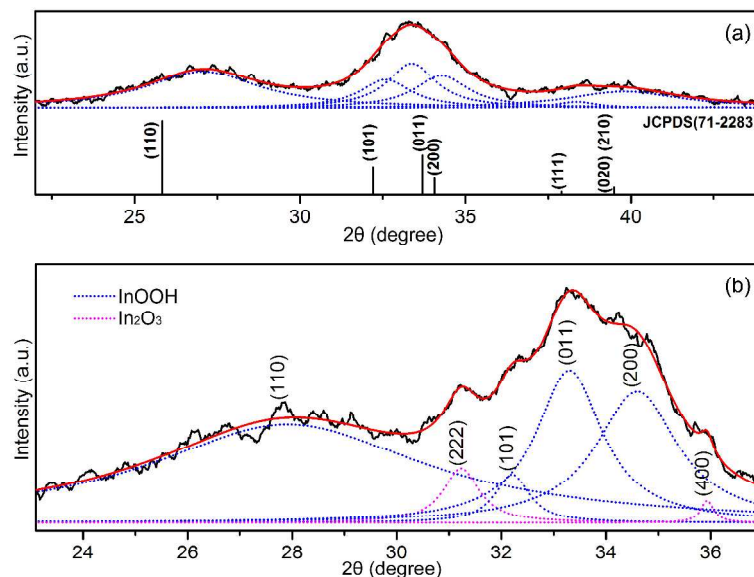


**Figure S1.** (a) The narrow-range XRD pattern of the sample synthesized at 160 °C with the heating rate of 4 °C/min (solid black trace), and the deconvoluted (110), (101), (011), (200), (111), (020) and (210) peaks of InOOH (dotted violet trace). The red trace is the superposition of the deconvoluted peaks. (b) The narrow-range XRD pattern of the sample synthesized at 130 °C with the heating rate of 8 °C/min (solid black trace), and the deconvoluted (222) and (400) peaks of *c*-In<sub>2</sub>O<sub>3</sub> (dotted pink trace), and (110), (101), (011) and (200) peaks of InOOH (dotted violet trace). The red trace is the superposition of the deconvoluted peaks.

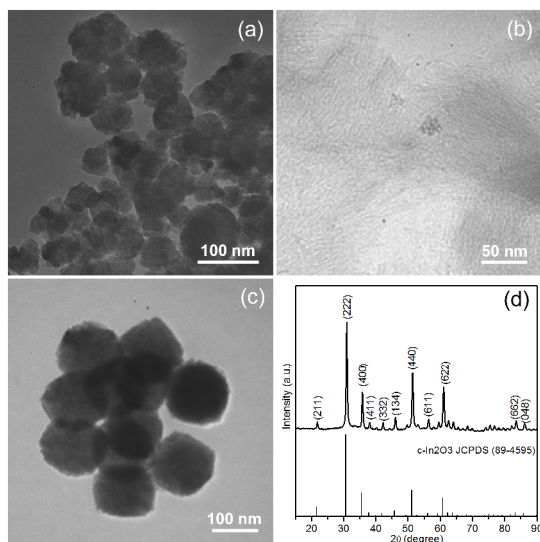


**Figure S2.** (a) The TEM image of  $\text{In}_2\text{O}_3$  nanoparticles synthesized at 200 °C with the heating rate of 4 °C/min. (b) The TEM image of the sample synthesized at 130 °C with the heating rate of 8 °C/min. (c, d) The TEM image and the XRD pattern of  $c\text{-In}_2\text{O}_3$  nanocubes synthesized at 190 °C with the heating rate of 8 °C/min.

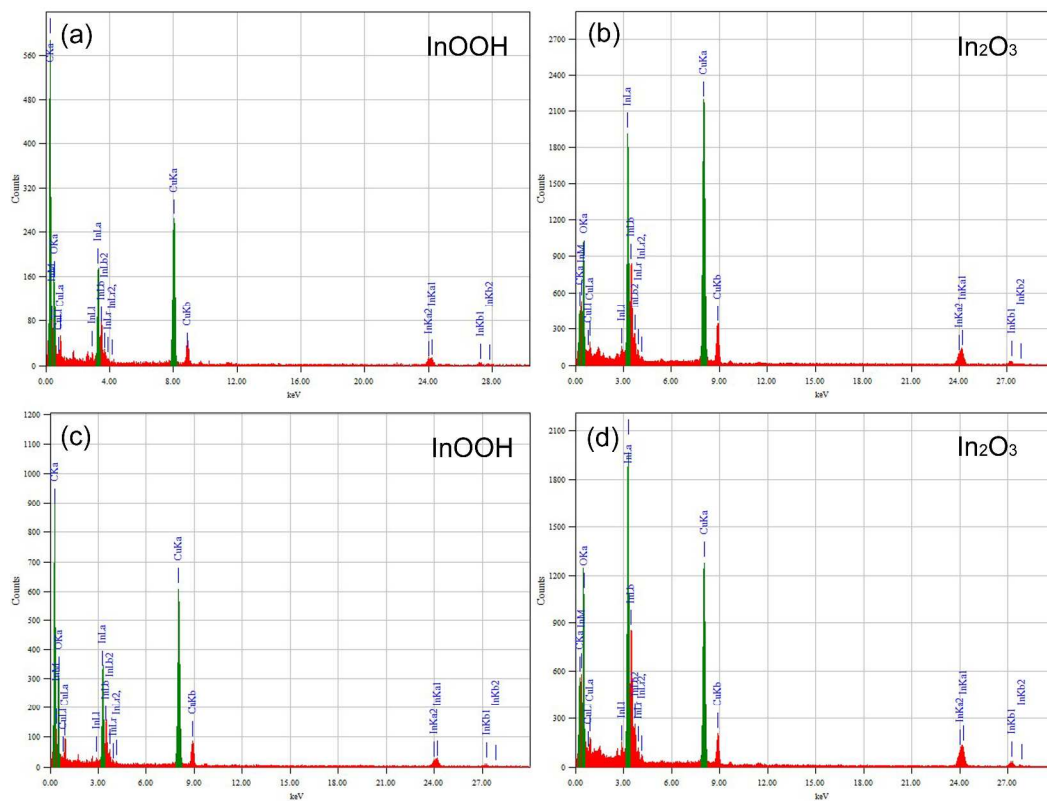


**Figure S3.** The EDS spectra of the InOOH and In<sub>2</sub>O<sub>3</sub> obtained at the heating rate of (a, b) 4 °C/min and (c, d) 8 °C/min, respectively.

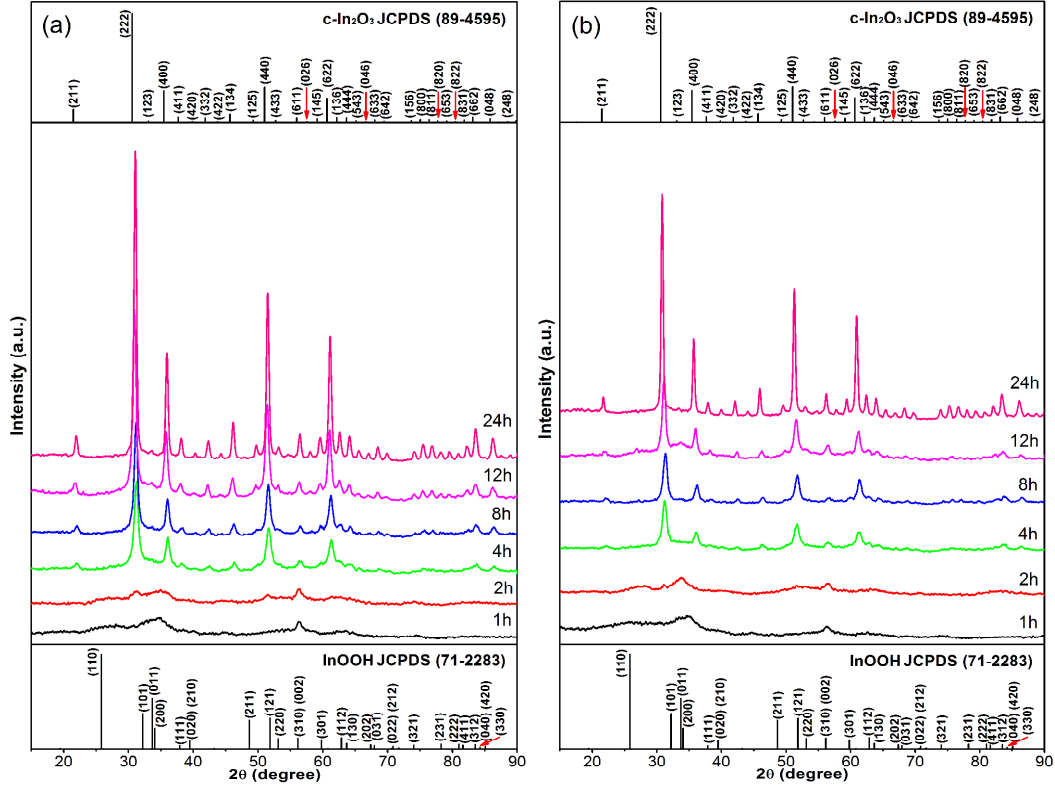


**Figure S4.** The XRD patterns of the samples hydrothermally treated with the heating rates of (a) 4 °C/min and (b) 8 °C/min for 1 h, 2 h, 4 h, 8 h, 12 h, and 24 h.

Because the sample is consisted of two phases (InOOH and  $c$ -In<sub>2</sub>O<sub>3</sub>), the weight ratio of each composition can be calculated using the following formula:

$$W_a = \frac{I_a / RIR_a}{I_a / RIR_a + I_b / RIR_b} \quad (1)$$

$$W_b = 1 - W_a \quad (2)$$

where  $I_a$  and  $I_b$  are integrated intensities of the strongest peak of  $c$ -In<sub>2</sub>O<sub>3</sub> and InOOH, respectively, the RIR values of InOOH (RIR = 8.31) and In<sub>2</sub>O<sub>3</sub> (RIR = 13.03) can be read from the matching PDF card in the database.

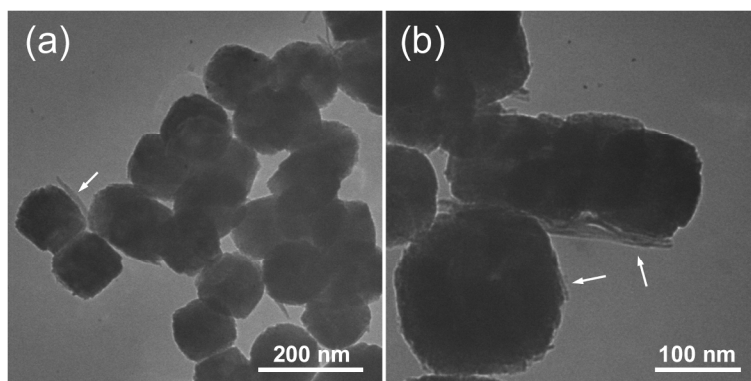


**Figure S5.** (a, b) The TEM images of the samples synthesized at 180 °C with the heating rate of 8 °C/min for 12 h

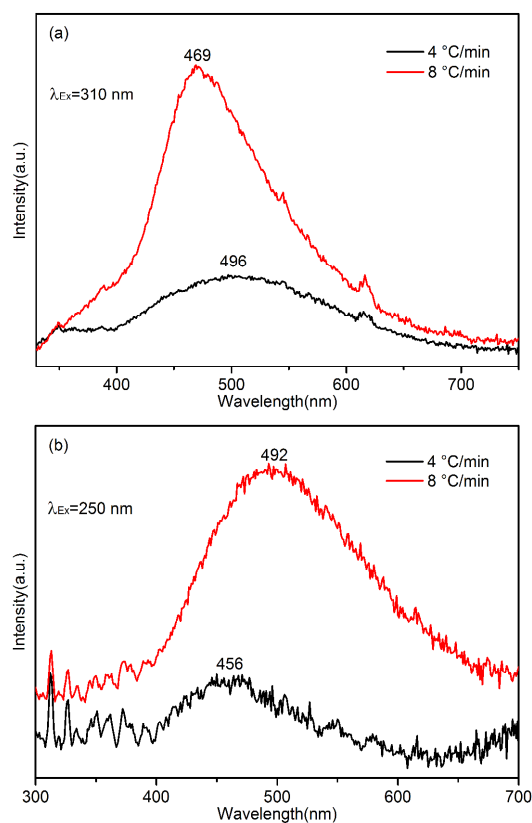


**Figure S6.** The photoluminescence spectra of (a) *c*-In<sub>2</sub>O<sub>3</sub> nanocubes and (b) InOOH nanowires synthesized at the different heating rates.

The photoluminescence (PL) spectra of the  $\text{In}_2\text{O}_3$  nanocubes and ultrathin  $\text{InOOH}$  nanowires prepared at different heating rates are shown in Figure S6. For both the  $\text{In}_2\text{O}_3$  nanocubes synthesised at different heating rates (Figure S6(a)), a broad emission band was observed in the visible regions with a 310 nm excitation wavelength. As compared to  $\text{In}_2\text{O}_3$  nanocubes obtained at the heating rate of 4 °C/min, the intensity of the emission band of  $\text{In}_2\text{O}_3$  nanocubes obtained at the heating rate of 8 °C/min is significantly strengthened, with the maximum of the emission band blue-shifting from 496 nm to 469 nm.

As a wide gap semiconductor, nanoscaled  $\text{In}_2\text{O}_3$  structures show PL emission at different wavelengths. The PL properties of  $\text{In}_2\text{O}_3$  affected by its dimensionality, shape, and size, as well as the synthetic process and parameters, have been widely reported.<sup>1,2</sup> The PL emission mechanism is still not clear. For the  $\text{In}_2\text{O}_3$  nanostructures, it is generally believed that the visible luminescence emission is mainly attributed to the existence of oxygen vacancies.<sup>2</sup> These oxygen vacancies normally act as deep defect donors in semiconductors and would induce the formation of new energy levels in the band gap. Thus, the increase in the PL intensity accompanied by the blue shift of the emission band can be attributed to higher density of oxygen vacancies and defects generated during the self-assembly process which happened at the heating rate of 8 °C/min.

For the ultrathin  $\text{InOOH}$  nanowires obtained at different heating rates (Figure S6(b)), a broad luminescence band in the visible range could be observed with a 250 nm excitation wavelength. Because the average size of the ultrathin  $\text{InOOH}$  nanowires is close to the Bohr diameter of the excitons, a few emission peaks in the UV region could be also observed and attributed to the quantum confinement effect. The visible luminescence emission is also due to the existence of vacancies and the  $\text{InOOH}$  nanowires obtained at the heating rate of 8 °C/min exhibit stronger PL

emission. However, red shift of the PL emission with increasing heating rate could be observed, which is quite different from the blue shift found in the PL spectra of  $\text{In}_2\text{O}_3$  nanocubes.

(1) Wang, C. Q.; Chen, D. R.; Jiao, X. L.; Chen, C. L. Lotus-Root-Like  $\text{In}_2\text{O}_3$  Nanostructures: Fabrication, Characterization, and Photoluminescence Properties. *J. Phys. Chem. C* **2007**, *111*, 13398–13403.

(2) Ko, T. S.; Chu, C. P.; Chen, J. R.; Lu, T. C.; Kuo, H. C.; Wang, S. C. Tunable Light Emissions from Thermally Evaporated  $\text{In}_2\text{O}_3$  Nanostructures Grown at Different Growth Temperatures. *J. Cryst. Growth* **2008**, *310*, 2264–2267.